Journal of Structural Geology 162 (2022) 104687

Contents lists available at ScienceDirect

Journal of Structural Geology

journal homepage: www.elsevier.com/locate/jsg

Tools to analyse misleading kinematic interpretations of faults offsetting inclined or folded surfaces: Applications to Asturian Basin (NW Iberian Peninsula) examples

Marta Magán *, Josep Poblet, Mayte Bulnes

Departamento de Geología, Universidad de Oviedo, C/Jesús Arias de Velasco s/n, 33005, Oviedo, EU, Spain

ARTICLE INFO

Keywords:
Faults
Inclined layers
Folds
Cross section
Map
Asturian basin

ABSTRACT

When working with geological maps and cross-sections, and no kinematic criteria on fault motion are available, we usually classify the type of fault (dip-slip, strike-slip, oblique) according to the observed separation of planar markers, usually bedding. Although in many cases the separation agrees with fault slip, and therefore, the deduced type of fault is correct, these deductions can be completely wrong in certain circumstances. Amongst other parameters, the observed separation depends on the angular relationship between the cut-off line of the planar marker on the fault plane and the slip vector. In this paper, we elaborate on this relationship and present a tool to facilitate classifications of faults whose motion does not involve rotation of the fault blocks, and cut and offset previously tilted or folded surfaces. This tool consists of graphs that predict how the observed separation will be in cross sections and maps. In addition, the influence of different parameters on the magnitude of the separation in a geological section across a fault is discussed. The validity of the presented tool is demonstrated through its application to two field examples of strike-slip faults offsetting inclined layers and a fold train in the Asturian Basin. Our graphs can be used to improve geological interpretations, in a predictive way when constructing geological maps and cross-sections, and to decipher the existence of layers tilted or folded before fault development.

1. Introduction

The most used classification of faults is based on their kinematics; when we know how two fault blocks have moved, we can state whether the fault is normal, reverse, left-lateral, right-lateral or oblique. Generally, the fault trace is an element easy to identify as it corresponds to a discontinuity. However, the direction and sense of fault displacement is usually more difficult to determine as, in many cases, no kinematic criteria are available (e.g., striations on the fault plane). It is even more complicated to estimate the net slip as two homologous points on both fault blocks need to be known. Nevertheless, it is common to quickly classify faults according to the offset we observe, even in the absence of clear kinematic criteria. For example, if a fault crops out on a vertical slope or cliff and the same layer appears at a higher elevation in the hanging wall than in the footwall, we conclude that the fault is reverse, while if the layer is located at a lower elevation in the hanging wall than in the footwall, we assume that the fault is normal. If on a geological map the fault hanging wall is formed by older rocks than those in the footwall, we conclude that the fault is reverse, while if they are younger, we assume that it is a normal fault. Thus, we usually base our fault classification on the observed separation of planar markers, in this case bedding, i.e., the distance between two parts of a horizon disrupted by a fault measured in a particular direction. These deductions are correct when the displaced marker is a horizontal surface before fault generation or it strikes to the same direction than the fault, however, when the planar marker had a previous dip and its strike is different from that of the fault, these deductions may be incorrect, and therefore, a classification based on separation may lead to incorrect structural interpretations (Fig. 1). This matter is particularly sensitive in the case of seismic profiles as data are 2D and it is difficult to obtain kinematic indicators. The concepts of slip and separation are well known from classical works of the past century (e.g., Reid et al., 1913; Straley, 1934; Crowell, 1959; Billings, 1972) and they have been extensively discussed in most Structural Geology books. One of the most interesting contributions on the separation and slip in faults is that of Ragan (2009). This author proposed constructing fault plane views in order to visualize the

* Corresponding author.
E-mail addresses: maganmarta@uniovi.es (M. Magán), jpoblet@uniovi.es (J. Poblet), maite@uniovi.es (M. Bulnes).

https://doi.org/10.1016/j.jsg.2022.104687
Received 4 March 2022; Received in revised form 21 July 2022; Accepted 22 July 2022
Available online 31 July 2022
0191-8141/© 2022 The Authors. Published by Elsevier Ltd. This is an open access article under the CC BY license (http://creativecommons.org/licenses/by/4.0/).

geometrical effects of the displacement and made an analysis of separation of a planar marker versus the cut-off line of the planar marker on the fault plane and the slip vector.

Working on coastal outcrops of Lower Jurassic rocks in the Asturian Basin, NW Iberian Peninsula, where some faults cut and offset inclined layers and kinematic criteria are available, we recognised faults whose separation disagrees with slip. This motivated us to recall this topic and discuss these relationships, create a tool to make easier the analysis of the relationship between slip and separation, and illustrate these situations using field examples. The tool consists of graphs relating the angle between the cut-off line of a surface on the fault plane and the slip vector. In addition, we have developed a Python script that plots field data on the graphs presented in this paper and constructs simple geological maps and sections across the faults, as well as fault plane views as proposed in Ragan (2009). Our analysis applies to faults whose motion does not involve rotation of the fault blocks, and is based on the current disposition of the elements displaced by the fault, but it does not consider whether the final disposition is due to a single fault motion event or due to fault reactivation.

The Asturian Basin, located in the northwestern portion of the Iberian Peninsula, is a Permian-Mesozoic extensional basin partially inverted during a Cenozoic contractional event. The Mesozoic extensional events led to folds related to normal faults, while the Cenozoic contractional event, which took place during the Alpine orogenesis, is characterised, among other structures, by reverse and strike-slip faults superimposed to Mesozoic structures (Lepvrier and Martínez-García, 1990; Uzkeda, 2013; Uzkeda et al., 2013, 2016). The angular relationships between the Mesozoic folds and the Cenozoic faults are very varied because the Mesozoic structures strike NE-SW, NW-SE and E-W. The Asturian coast contains exceptional top-views and cross-sectional exposures of the emerged portion of the Asturian Basin by the Cantabrian Sea (Martín et al., 2013; Uzkeda et al., 2018, 2022). The excellent quality outcrops combined with the use of traditional and digital geological mapping, as well as the construction and interpretation of virtual outcrop models (Xu et al., 2000) of this region has allowed us to perform a high-resolution geological analysis. This approach has provided measurements and observations at different scales and bed-by-bed resolution, so that we are able to identify the same layers and structures in both fault blocks. This makes it possible to determine without any uncertainty the type of fault and estimate the dip and strike separations, i.e., the distance of formerly adjacent beds on either side of a fault surface, measured along the dip of the fault or measured along strike of the fault respectively.

The most common way to proceed in order to determine the different cases resulting from the interaction of two elements consists of modifying one element, the other, and finally both. Although apparently in the study of relationships between faults and layers there are only two elements, unfortunately, there are too many parameters to be considered, both in the case of faults (orientation, type of fault according to its displacement, magnitude of displacement, etc.) and in the case of tilted/folded layers (orientation of beds, axial surfaces and fold axes, interlimb angle, fold geometry, etc.), to analyse their effect one by one. In this paper, we will check how the variation of the parameters, which we consider most important, influences our perception of the type of fault. First, we will examine a simple and, in our opinion, very illustrative case, since it may be relatively common for a geologist to map faults in the field that cut and offset layers with a certain previous dip. Next, we will explore what happens when faults cut and offset folds. We will show different implications derived from the modification of the different parameters related to faults and layers using sections and geological maps, since they are two of the most used techniques in Geology to represent the geometry of geological bodies.

2. Faults displacing previously inclined layers

In this section, we analyse the most important parameters that influence the dip and strike fault separation that one can see in cross section and in map respectively, as well as derived implications from variation of these parameters. Finally, we present a perfectly bounded field example and two theoretical examples.

2.1. Geological cross-sections and maps

In a region where layers exhibit a normal polarity and are horizontal or their strike is the same than that of the fault, the sense of dip separation shown in a section across the fault is consistent with the slip of the fault. That is, in dipping faults, reverse faults place hanging wall older rocks over footwall younger rocks, normal faults place hanging wall younger rocks over footwall older rocks, and strike-slip faults cause no dip separation. However, in those cases where bedding was tilted before fault development and its strike is not parallel to that of the fault, the fault may show confusing dip separations (Fig. 1). Thus, a reverse fault may appear as a normal fault or vice versa, and a strike-slip fault may appear as a reverse or normal fault. To show how the fault dip separation would look like in cross sections perpendicular to the fault strike, we have constructed a graph (Fig. 2b). In this graph, we have represented the different types of faults according to their kinematics based on the pitch of the net-slip vector (or in other words, the pitch of linear kinematic indicators, such as fault striations, on the fault surface) as a function of bedding cut-off lines on the fault plane. The parameters used in this graph are illustrated in Fig. 2a. The analysis of this graph has allowed us to draw the conclusions set out below.

1) If the slip vector and the bedding cut-off lines are parallel, any fault, irrespective of the type of fault (reverse, normal, strike-slip or oblique), will appear as a strike-slip fault in cross section, i.e., same age hanging wall and footwall rocks will be located at the same height, and therefore, the fault dip separation will be zero (Fig. 1a, blue lines in Fig. 2b). In all other cases, however, the faults will show normal or reverse dip separation.
2) Dip-slip, oblique-slip and strike-slip faults with a normal component will show normal dip separation except when the slip vector pitches in the same direction than the bedding cut-off lines at a smaller angle (measured from 0° to 90°) than that of the bedding cut-off lines.

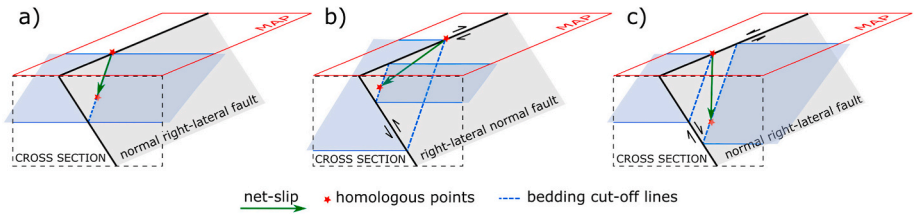

Fig. 1. Block diagrams illustrating faults offsetting beds tilted before fault development. a) Normal right-lateral fault whose dip and strike separation are null because the net-slip vector and the bedding cut-off lines are parallel, and therefore, the fault causes apparently no bed offset in cross-sectional and map views. b) Right-lateral normal fault that appears as a reverse fault in cross-sectional view and as a right-lateral fault in map view because the net-slip vector and the bedding cut-off lines pitch in the same direction, but the net-slip pitch is lesser than that of the bedding cut-off lines. c) Normal right-lateral fault that appears as a normal fault in cross-sectional view and as a left-lateral fault in map view because the net-slip vector and the bedding cut-off lines pitch in the same direction, but the net-slip pitch is greater than that of the bedding cut-off lines.

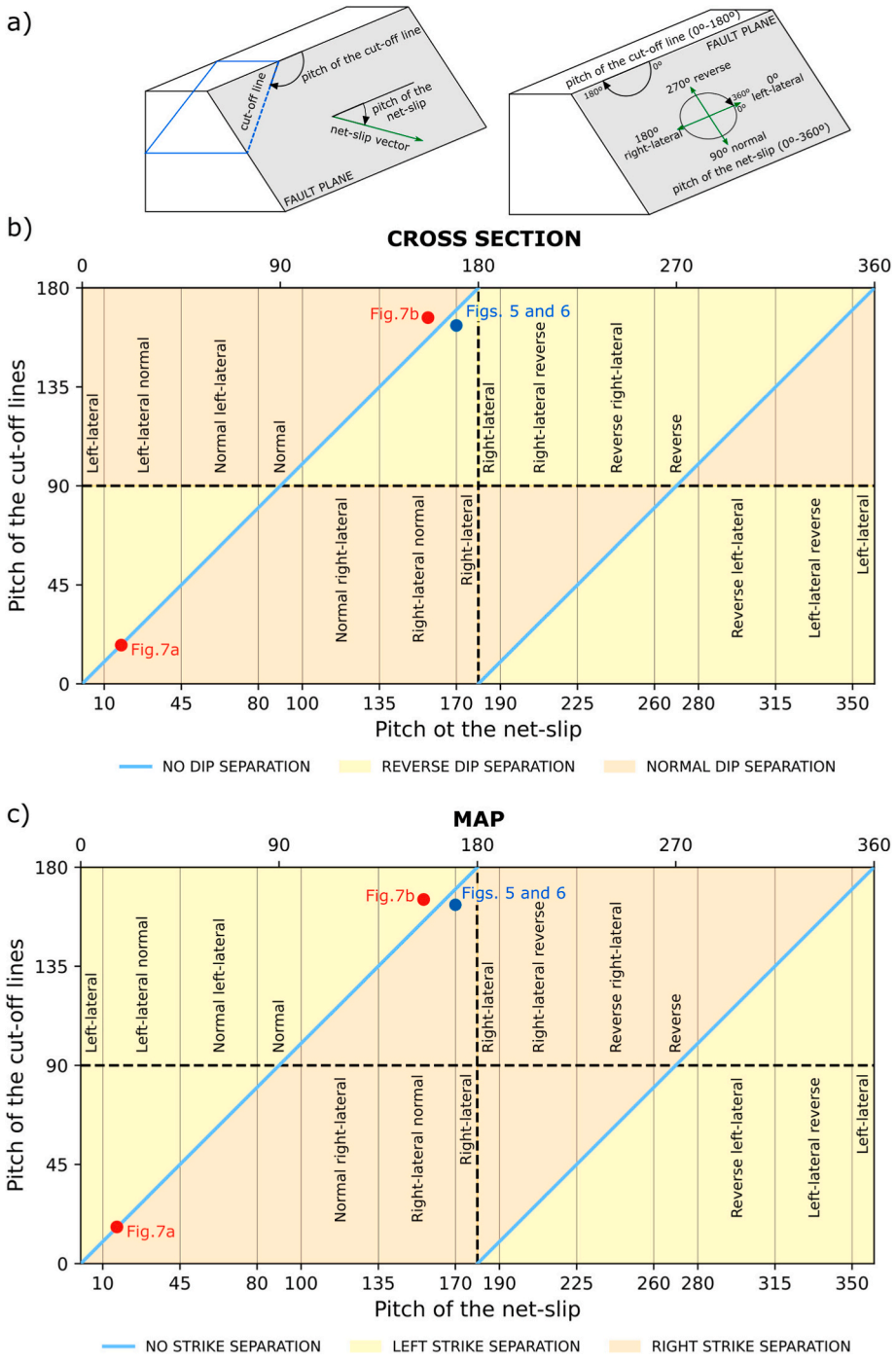

Fig. 2. Graphs showing the pitch of the net slip on the fault versus the pitch of bedding cut-off lines on the fault plane. a) Sketch illustrating the parameters used in the graphs b) and c) and their possible values. Pitch is measured clockwise. To facilitate the data projection on the graphs, the net-slip pitch has been assigned a range between 0° and 360°, while the pitch of the bedding cut-off lines has been assigned a range between 0° and 180°. However, when we use the term pitch in the text, we assume it ranges from 0° to 90°. b) Graph showing the fields of dip separation (normal, reverse or no separation) for cross-sectional view. c) Graph showing the fields of strike separation (left, right or no separation) for map view. The blue dots plotted in figures b) and c) correspond to the fault shown in Fig. 5 and 6, whereas the red dots correspond to the faults shown in Fig. 7. In figures b) and c), the different types of faults according to their kinematics are separated by thin black vertical lines. (For interpretation of the references to colour in this figure legend, the reader is referred to the Web version of this article.)

Similarly, dip-slip, oblique-slip and strike-slip faults with a reverse component will show reverse dip separation except when the slip vector pitches in the same direction than the bedding cut-off lines at a smaller angle than that of the bedding cut-off lines (Figs. 1b and 2b).

Similarly to cross-sections, in geological maps there are also cases where the fault strike separation disagrees with the fault slip. We have constructed a graph to show how the fault strike separation would look like in maps (Fig. 2c). In this graph, we have represented the different types of faults according to their kinematics based on the pitch of the net-slip vector (i.e., the pitch of linear kinematic indicators such as fault striations) versus the pith of the bedding cut-off lines on the fault plane.

Different situations, briefly described below, occur.

1) If the fault slip vector and the bedding cut-off lines are parallel, any type of fault (reverse, normal, strike-slip and oblique) will show no strike separation, so that it will appear on the map as if the fault caused no movement (Fig. 1a). In all other cases, faults will display strike separations other than zero (Fig. 2c).
2) Apart from the case described above, faults will show strike separations consistent with fault slip except when the fault slip vector pitches in the same direction than the bedding cut-off lines at a greater angle than that of the bedding cut-off lines, then the fault strike separation will disagree with the fault slip. Thus, a fault with a left-lateral component will exhibit a right strike separation on the

map, whereas a fault with a right-lateral component of motion will appear as a fault with left strike separation on the map (Figs. 1c and 2c).

To visualize the particular case of pure strike-slip faults, we have created a diagram including maps and cross sections that takes into account fault dip and bedding dip, and whether faults are right-lateral or left-lateral (Fig. 3).

Two particular cases need to be explained separately.

1) In relation to the dip of the faults. Vertical faults have neither hanging wall nor footwall. Fault block motion in vertical faults is usually identified using cardinal points instead of the classical classification of normal or reverse faults (although they can still be labelled as right or left-lateral faults), and therefore, the graphs in Fig. 2 are not appropriate for vertical faults. Horizontal faults, although they do have hanging wall and footwall, their movement refers to cardinal points instead of the classical classification of normal, reverse, etc. faults. Again, the graphs in Fig. 2 do not seem to be appropriate for horizontal faults. To be able to plot these faults in

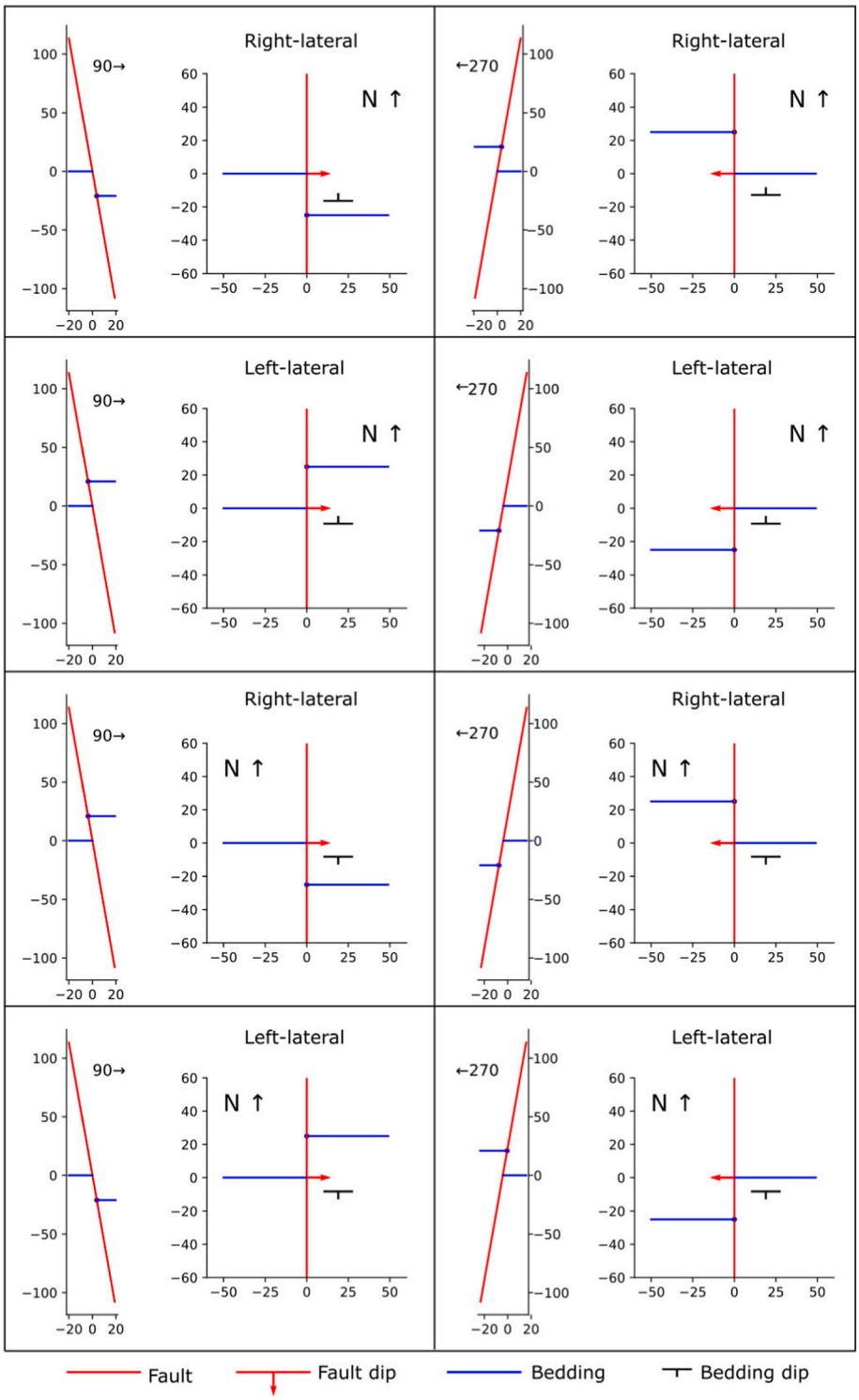

Fig. 3. Diagram showing how pure right-lateral and left-lateral strike-slip faults appear in cross section and map as a function of fault dip and layers dip. The cross sections are represented on the left part of each cell, whereas the maps are on the right side. For simplicity, faults are assumed to strike N–S and layers E-W. Bedding dip may vary from quasi-vertical to quasi-horizontal. The fault illustrated in Fig. 5 and 6 corresponds to the example shown in the upper right corner. This figure has been constructed using the outputs of the Python script developed assuming a fault net-slip of 25 units and a bedding dip of 40°.

Fig. 2 graphs we suggest assuming that vertical faults are not strictly vertical, but have a dip of 89.9°, while horizontal faults would be assigned a dip of 0.1°. Since natural fault surfaces are usually not perfect planes but rather irregular surfaces, this assumption seems reasonable.

2) In relation to the orientation of the layers. When the layers are parallel to the observation plane, i.e., to the section plane in the case of geological cross-sections or to the map plane in the case of geological maps, then different layers appear in both fault blocks. Unfortunately, in these cases it is impossible to determine neither the dip separation nor the strike separation, and therefore, the graphs in Fig. 2 cannot be used.

In order to determine the influence of different parameters on the magnitude of dip separation, we will consider a simple case of a vertical strike-slip fault that offsets a previously dipping bed whose dip ranges from more than 0° to less than 90°. Since it is impossible to examine all possible situations, we will vary three different parameters and analyse qualitatively the behaviour of these variations. To do so, we will use a dip separation versus strike separation graph for different pitch values of bedding cut-off lines on the fault plane (Fig. 4). The parameters we will modify are the angle between the fault strike and the bedding strike, the dip of the layers, and the fault slip (or separation, as it is a pure strike-slip fault and its strike separation coincides with slip). The conclusions obtained are listed below.

1) When the angle between the bedding strike and the fault strike decreases, keeping constant the bedding dip and the fault slip, then the pitch of the bedding cut-off lines decreases and the dip separation we see in cross section decreases as well (path illustrated by green arrows in Fig. 4a and b).
2) When the bedding dip increases, keeping constant the angle between the bedding strike and the fault strike as well as the fault slip, then the pitch of the bedding cut-off lines increases and the dip separation we see in cross section also increases (path illustrated by blue arrows in Fig. 4a and b).
3) When the fault slip increases, keeping constant the angle between the bedding strike and the fault strike as well as the bedding dip, the pitch of the bedding cut-off lines remains constant but the dip separation viewed in cross section increases (path illustrated by red arrows in Fig. 4a and b).

The conclusions explained above derive from cases in which we only vary one of the parameters and the rest remain constant. However, from the graph in Fig. 4a, conclusions can be drawn for cases in which more than one parameter varies. For instance, for the same increase in strike separation, the larger the pitch of the cut-off lines on the fault surface the larger the dip separation increase.

2.2. Field example

The selected field example is located in the southeastern part of Peñarrubia Beach, Gijón (Asturias) by the Cantabrian Sea (Fig. 5a). The Jurassic rocks that crop out in the Peñarrubia Beach belong to the northern part of the emerged portion of the Asturian Basin and consist of alternations of limestones and marls. In this region, mapped in Beroiz et al. (1972), Gutiérrez Claverol et al. (2002), Merino-Tomé et al. (2014) and Odriozola (2016), there is an E-W to WNW-ESE fault, whose trace is approximately rectilinear in map view and reaches a few hectometres length along strike (Fig. 5b). The fault surface dips steeply to the SSW (Fig. 6a), although locally it can dip to the NNE (Fig. 5d). This fault offsets a N–S syncline causing a right strike separation on the geological map (Fig. 5b). Low-pitch slickensides (18° W) recognised on the fault surface indicate right-lateral slip with a small normal component (Fig. 5d). To estimate the net-slip value and its pitch on the fault surface, one fault-parallel section across the hanging wall and another across the footwall have been constructed both adjacent to the fault (dashed blue and red lines in Fig. 5b). Both sections have been overlapped using a reference point of known coordinates in order to construct an Allan map (Allan, 1989) (Fig. 5e). The hinge of the syncline developed at the same horizon in both fault blocks has been taken as homologous points in the Allan map. The distance between these two homologous points on the Allan map is the net slip and its dip is the pitch of the net slip. The net slip obtained is 38.7 m, the strike slip is 38.1 m, the dip slip is about 4.4 m and the pitch of the net slip is almost 9.5° to the W, i.e., it is a strike-slip fault. The net-slip pitch and the fault motion sense calculated using homologous points on both fault blocks depicted in the Allan map (Fig. 5e) coincide with the pitch and direction of movement deduced from the slickensides measured on the fault plane in the field (Fig. 5d). The calculated net-slip pitch and the pitch measured in the field using kinematic indicators are not identical because the pitch of the slickensides corresponds to values measured at specific locations and neither the fault surface is a perfect plane nor the slickensides are perfectly rectilinear, and because the calculated net-slip corresponds to the final displacement vector that may be the result of the sum of different fault motion pulses with similar orientation slickensides but not strictly parallel. Thus, both the theoretical calculations and the kinematic indicators, clearly show that this fault is an almost pure right-lateral strike-slip fault with a slight normal component. However, on the coastal cliff, which is approximately vertical and almost perpendicular

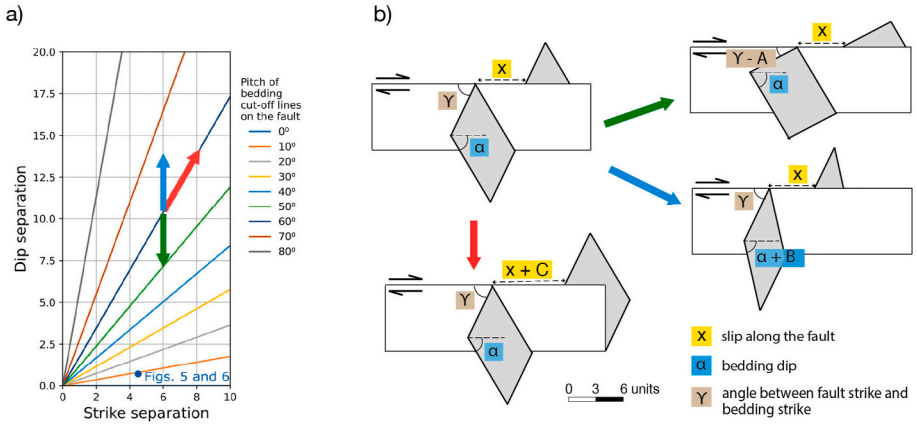

Fig. 4. a) Graph illustrating dip separation versus strike separation for different pitches (from 0 to 80°) of bedding cut-off lines on the fault plane in the case of a vertical strike-slip fault. To use this graph, if the strike separation of the fault to be analysed is greater than 10, divide the measured strike separation by 10 or multiples of 10 to obtain a value between 0 and 10, plot on the graph the new strike separation and the pitch of the bedding cut-off lines on the fault, and apply the inverse operation to the resulting dip separation to obtain the actual dip separation. The blue dot corresponds to the fault illustrated in Fig. 5 and 6. The meaning of the three arrows is explained in b). b) Sketches illustrating the path of the green (decrease in the angle between the fault and bedding strikes), blue (increase in layer dip) and red (increase in the fault strike separation) arrows plotted in figure a). Letters A, B and C are positive values. (For interpretation of the references to colour in this figure legend, the reader is referred to the Web version of this article.)

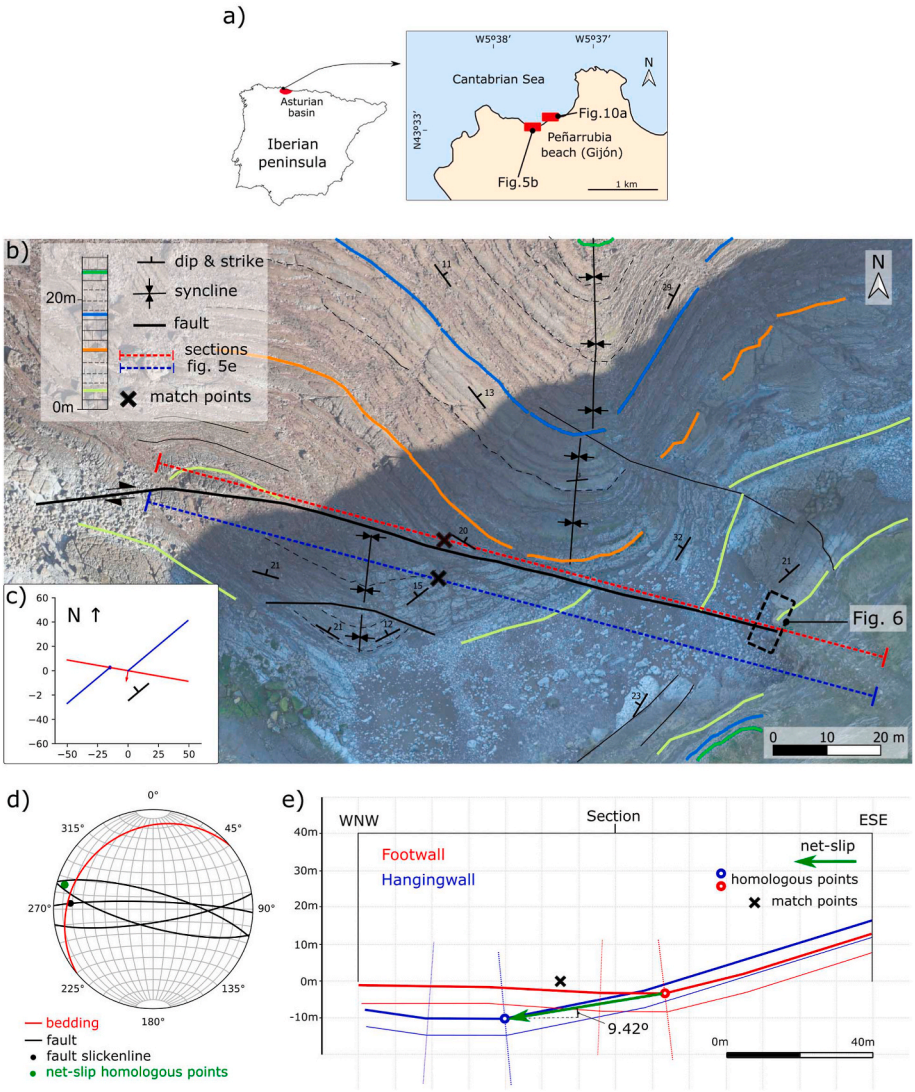

Fig. 5. a) Maps showing the location of the field examples. b) Photogeological interpretation of an orthophotograph showing a WNW-ESE right-lateral strike-slip fault cutting and offsetting a N–S syncline. c) Simplified geological map that simulates the fault depicted in b) (red line) cutting and offsetting a previously dipping horizon (blue lines). This figure has been constructed using an output of the Python script developed and employing field data as input data. d) Equal-area projection of measurements related to the fault illustrated in b), constructed with a Python script. e) Two overlapped geological sections parallel to the fault illustrated in b). The cross-section lines are located in b). These cross-sections have been constructed employing the dip domains (or kink) method. The small black cross indicates the match point used to assemble both geological sections. The thick and thin red horizons in the fault footwall are the same ones than the thick and thin blue horizons in the fault hanging wall, and the syncline involving the red horizons is the same one than the syncline involving the blue horizons. (For interpretation of the references to colour in this figure legend, the reader is referred to the Web version of this article.)

to the fault strike, this fault appears as a reverse fault with a dip separation of approximately 1.5 m (Fig. 6a). The calculated pitch of the net slip, the pitch of the bedding cut-off lines on the fault plane (estimated on the equal-area projection illustrated in Fig. 5d using bedding and fault field measurements), as well as the calculated value of strike separation, have been plotted on the graphs in Figs. 2 and 4. The graphs in Fig. 2, the map and cross section outputs of the Python script (Figs. 5c and 6b) and the diagrams shown in Fig. 3 confirm that the fault analysed, despite being an almost pure right-lateral strike-slip fault with a slight normal component, should appear as a reverse fault in cross section, while the graph in Fig. 4a and the cross section derived from the Phyton script (Fig. 6b) confirm that its dip separation should be around 1.5 m as shown in the field photograph depicted in Fig. 6a.

2.3. Theoretical examples

In order to show examples of faults whose motion does not cause displacement of the layers on the map, or causes apparent displacement of the layers on the map contrary to the actual fault motion, geological cross-sections and maps of two theoretical examples constructed with the Python script developed are presented below.

The first example is a left-lateral fault with a slight normal component (equal-area plot in Fig. 7a). The bedding cut-off lines on the fault plane are almost parallel to the net slip, as shown by the plot of the fault data on the graphs in Fig. 2b and c. This causes that, regardless of the magnitude of motion along the fault, this fault does not offset the layers neither in the geological cross-section nor in the geological map (Fig. 7a).

The second example is a right-lateral fault with a slight normal component (equal-area plot in Fig. 7b). The pitch of the bedding cut-off lines on the fault plane is greater than the pitch of the net slip, as shown by the data plotted on the graphs in Fig. 2b and c. Thus, although in the geological cross-section the fault shows a small normal dip separation consistent with the actual net-slip, on the geological map it exhibits a left strike separation although the fault is really right-lateral (Fig. 7b).

3. Faults displacing previously folded layers

3.1. Geological maps

Imagine a region where cylindrical folds, with axes parallel to the strike of the axial planes, are cut and offset by a fault whose strike is parallel to the axial plane strike and the dip of both the axial planes and the fault are constant along strike. In this particular situation, the fault maintains the same character along its entire trace, i.e., the geological map shows a fault in which the oldest rocks are always in one fault block and the youngest rocks in the other. However, in other cases there may be segments of the same fault where the oldest rocks are in one fault

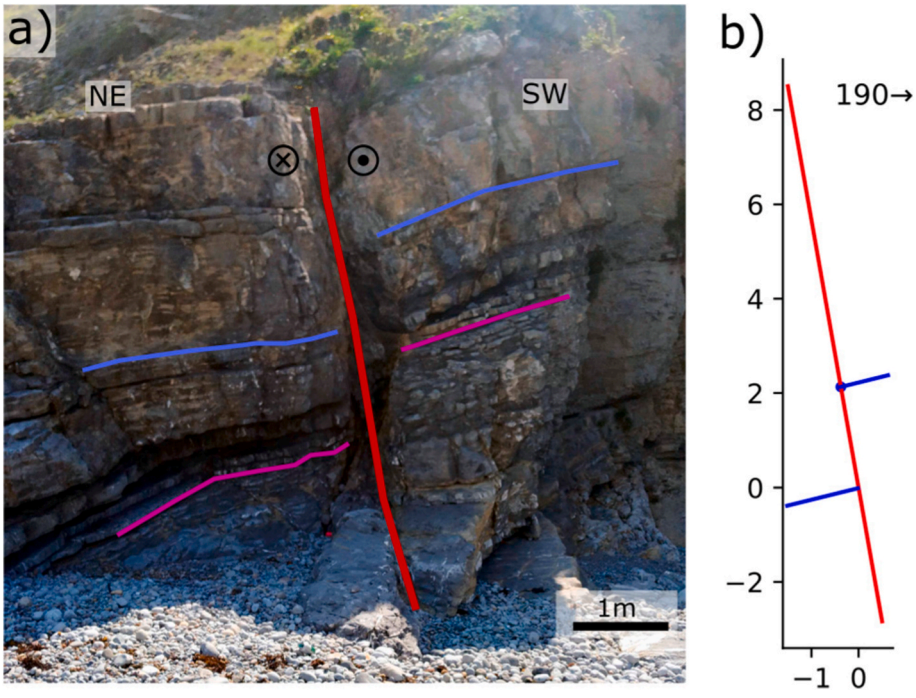

Fig. 6. a) Photogeological interpretation of a cliff showing the fault displacement produced by the right-lateral fault illustrated in Fig. 5 on a subvertical cross-sectional view almost perpendicular to the strike of the fault. b) Geological cross-section that simulates the fault (red line) depicted in Fig. 5 cutting and offsetting a previously dipping horizon (blue lines). The cross section is perpendicular to the strike of the fault. This figure has been constructed using the outputs of the Python script developed and employing field data as input data. (For interpretation of the references to colour in this figure legend, the reader is referred to the Web version of this article.)

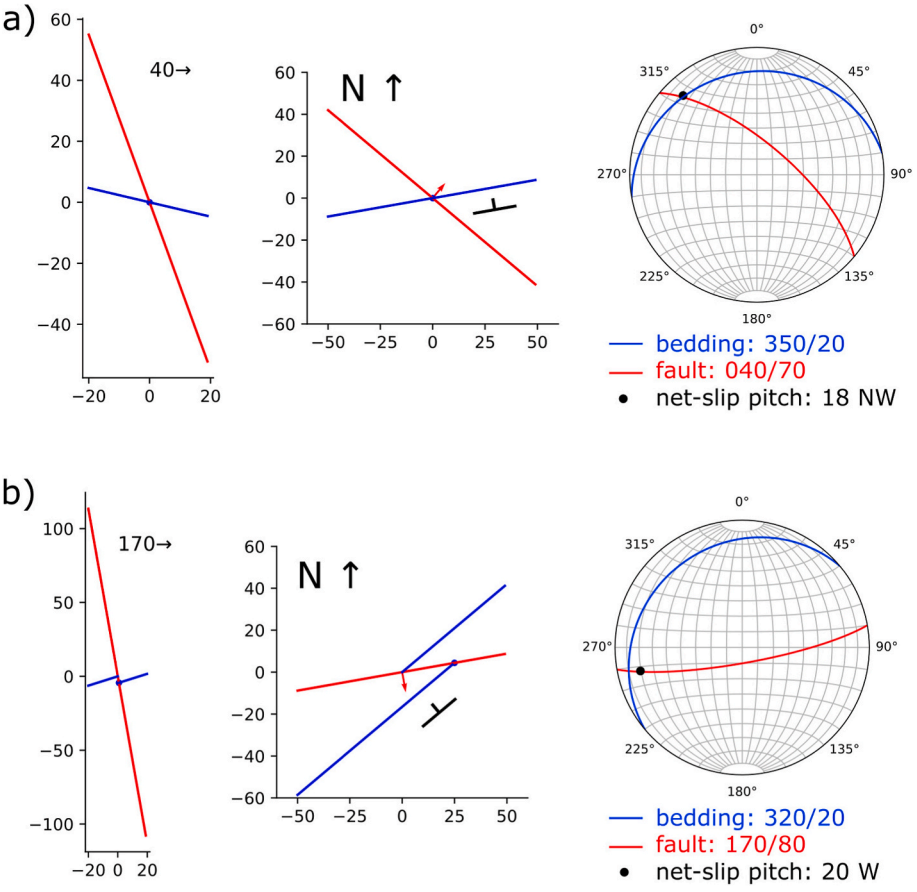

Fig. 7. a) and b) Geological cross-sections and maps of two faults (red lines) that cut and offset a previously dipping horizon (blue lines). The direction of the cross sections is perpendicular to the strike of the faults. The fault in figure a) is a left-lateral strike-slip fault, whereas the fault in figure b) is a right-lateral strike-slip fault as shown in the equal area plots. The geological cross-sections and maps exhibit no strike separation in the case of figure a), and a normal dip separation and a left strike separation in the case of figure b) as predicted by the graphs in Fig. 2b and c. The cross sections and maps have been constructed using the outputs of the Python script developed, whereas the equal-area plots have been constructed with a Python script. (For interpretation of the references to colour in this figure legend, the reader is referred to the Web version of this article.)

block and segments where the oldest rocks are in the other fault block. To illustrate these situations in map view, we have assumed that the folds have a kink-chevron geometry and we have constructed a graph (Fig. 8) in which the x axis represents different types of faults according to their kinematics based on the pitch of the slip vector (i.e., kinematic indicators), and the y axis is the pitch of the axial planes cut-off lines on the fault plane. The following conclusions can be drawn from the analysis of this graph.

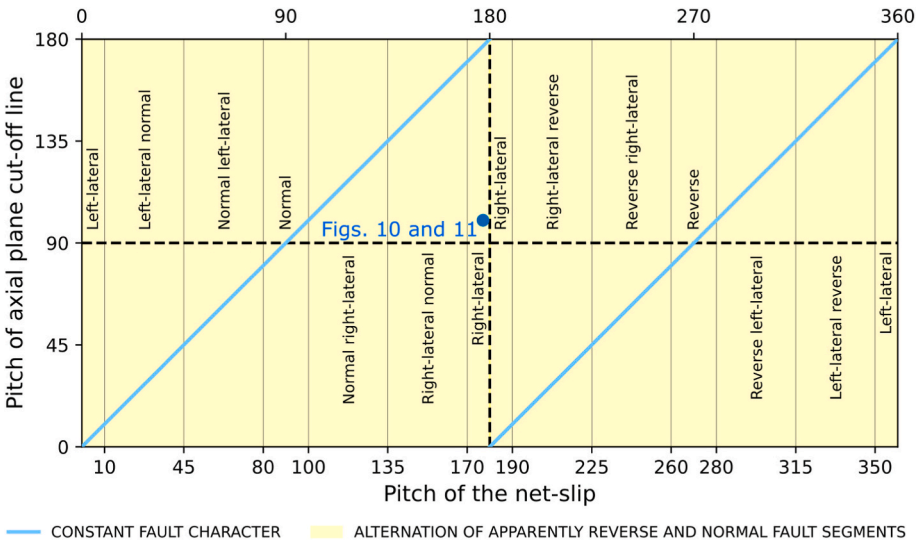

Fig. 8. Graph showing whether faults have apparently reverse/normal segments or not as a function of the pitch of the net slip (or kinematic indicators) on the fault versus the pitch of axial plane cut-off lines on the fault plane. The parameters used in this graph are illustrated in Fig. 2a. To facilitate the data projection on the graph, the net-slip pitch has been assigned a range between 0° and 360°, while the pitch of the axial plane cut-off lines has been assigned a range between 0° and 180°. However, when we use the term pitch in the text, we assume it ranges from 0° to 90°. The different types of faults according to their kinematics are separated by thin black vertical lines. The blue dot corresponds to the projection of the fault shown in Fig. 10 and 11. (For interpretation of the references to colour in this figure legend, the reader is referred to the Web version of this article.)

1) Regardless of the type of fault considered, when the slip vector and the axial plane cut-off lines are parallel, the faults maintain the same character along strike on a geological map (blue lines in Fig. 8).

2) In all other cases, regardless of the fault type, the faults may have segments where older rocks are located in one fault block and younger rocks in the other, and segments where the opposite situation occurs. Those fault segments where older rocks are in the

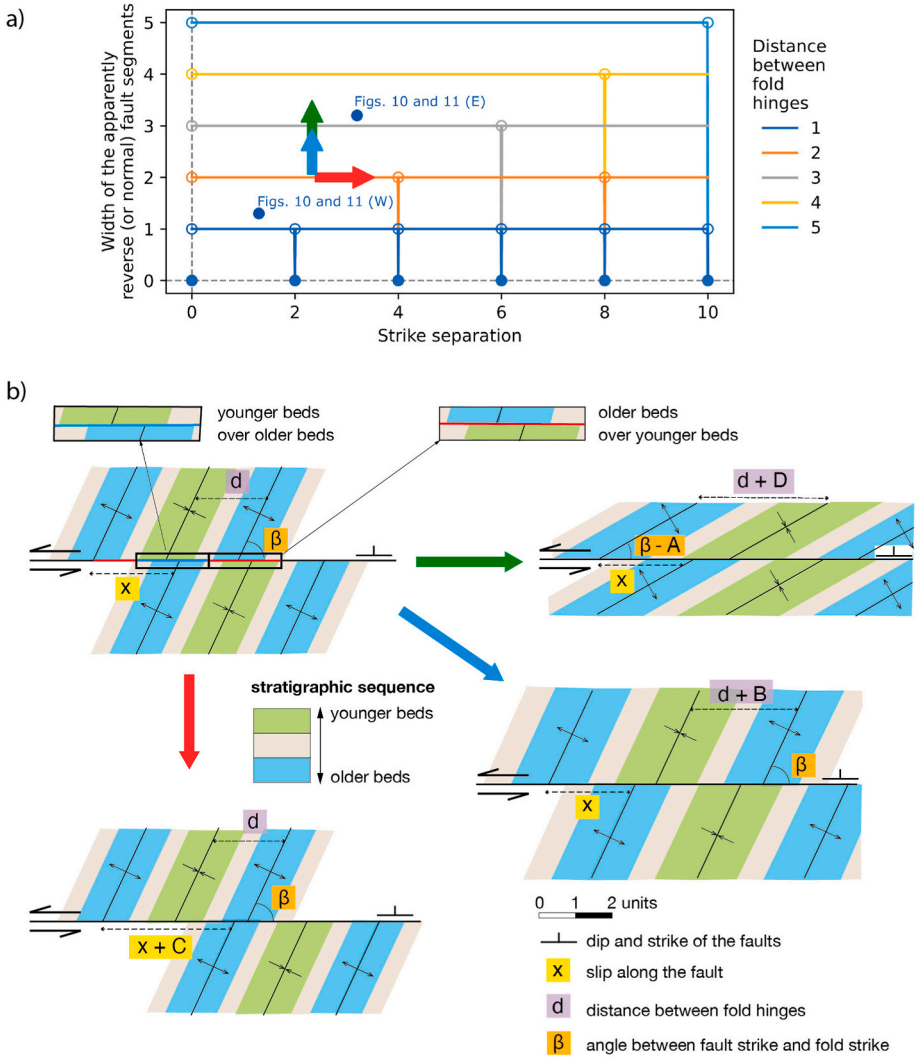

Fig. 9. a) Graph illustrating the width of the apparently reverse/normal fault segments versus the strike separation for different distances between fold hinges in the case of a vertical strike-slip fault that offsets a fold train of upright, equally spaced folds. When the strike separation is a multiple of twice the fold hinge spacing, the fault appears to have no displacement. To use this graph, if the strike separation of the fault to be analysed is greater than 10, divide the measured strike separation and the distance between fold hinges by 10 or multiples of 10 to obtain a value between 0 and 10, plot the new strike separation and the distance between fold hinges on the graph, and apply the inverse operation to the resulting width of the apparently reverse/normal fault segments to obtain the actual value. The blue dots correspond to the east and west parts of the fault illustrated in Fig. 10 and 11. The meaning of the three arrows is explained in b). b) Sketches illustrating the path of the green (decrease in the angle between fault strike and folds), blue (increase in the distance between the fold hinges measured parallel to the fault) and red (increase in the fault strike separation) arrows plotted in figure a). Letters A, B, C and D are positive values. (For interpretation of the references to colour in this figure legend, the reader is referred to the Web version of this article.)

hanging wall and younger ones in the footwall exhibit an apparent reverse displacement, whereas those fault segments where younger rocks are in the hanging wall and older ones in the footwall exhibit an apparent normal displacement (Fig. 8). In the case of strictly vertical faults, since there is no hanging wall and footwall, we could only speak of younger or older rocks in one or the other fault block.

There are many parameters that influence the width of the apparently reverse fault segments and that of the apparently normal fault segments along the same fault, and therefore, it is difficult to consider all the different situations. Thus, we propose to explore a simple case; a fold train formed by equally spaced anticlines and synclines with horizontal fold axes and vertical axial surfaces cut and offset by a pure strike-slip fault. The folds are cylindrical, their geometrical features are identical and the topographical surface is flat. The results will be shown using a graph which relates the width of the apparently reverse and apparently normal fault segments versus the fault strike separation for different distances between fold hinges measured parallel to the fault (Fig. 9). The basic parameters we will modify are the angle between the fault strike and the folds, the fault displacement, and the distance between fold hinges measured parallel to the fault trace. The results derived from the graph analysis are briefly explained below.

1) If we keep constant the fault strike separation but the angle between the fault strike and the folds decreases, then the distance between fold hinges measured parallel to the fault trace increases, so that the width of the apparently reverse and normal fault segments increases as well (path illustrated by green arrows in Fig. 9a and b).
2) When the distance between fold hinges increases, keeping constant the fault strike separation, as well as the angle between the fault strike and the folds, then the width of the apparently reverse and normal fault segments increases (path illustrated by blue arrows in Fig. 9a and b).
3) When the fault strike separation increases, keeping constant the angle between the fault strike and the folds, as well as the distance between fold hinges, the width of the apparently reverse and normal fault segments remains constant, except when the fault strike separation is a multiple of twice the distance between fold hinges; in this particular case the fault appears to have no strike separation (path illustrated by red arrows in Fig. 9a and b).

3.2. Field example

The fault we will analyse in this section is located a few hundred metres farther north than the fault described above (Fig. 5a). It has an E-W to WNW-ESE strike and very steep dip both towards the N and S (Fig. 10), predominantly towards the S, and cuts and offsets a NNE-SSW fold train. This fault displays a slightly corrugated map trace and hectometric length along strike (Fig. 10a). The low pitch slickensides identified on the fault surface, together with some right-lateral shear zones, indicate right-lateral fault motion (Fig. 10b). According to the geological map (Fig. 10a), the axial trace of the westernmost NNE-SSW fold is curved near the fault, which is interpreted as a drag fold consistent with a right-lateral fault movement. We have calculated the coordinates of the intersection point between the fault and an axis of an anticline developed in a horizon located in the north fault block, and the coordinates of the intersection point between the fault and the same fold developed in the same horizon in the south fault block. Since these two points correspond to homologous points in both fault blocks, this has made it possible to determine the fault net-slip, its pitch and the fault motion sense. The calculated net-slip is 33.5 m, the strike slip is almost 33.5 m, the dip slip is slightly greater than 1 m and the net-slip pitch is almost 2.3° (Fig. 10c); thus, the fault is a strike-slip fault, in particular a right-lateral fault. The net-slip pitch and the sense of fault movement obtained using homologous points on the two fault blocks (Fig. 10c), coincide with the pitch and direction of movement obtained from the kinematic indicators measured in the field (Fig. 10b). As in the case of the fault described above, the calculated pitch of the net slip and that of the kinematic indicators measured in the field are not identical because the slickensides have been measured in different locations and the fault surface is not a perfect plane, and because the calculated net-slip is the final displacement vector that may result from the sum of different fault

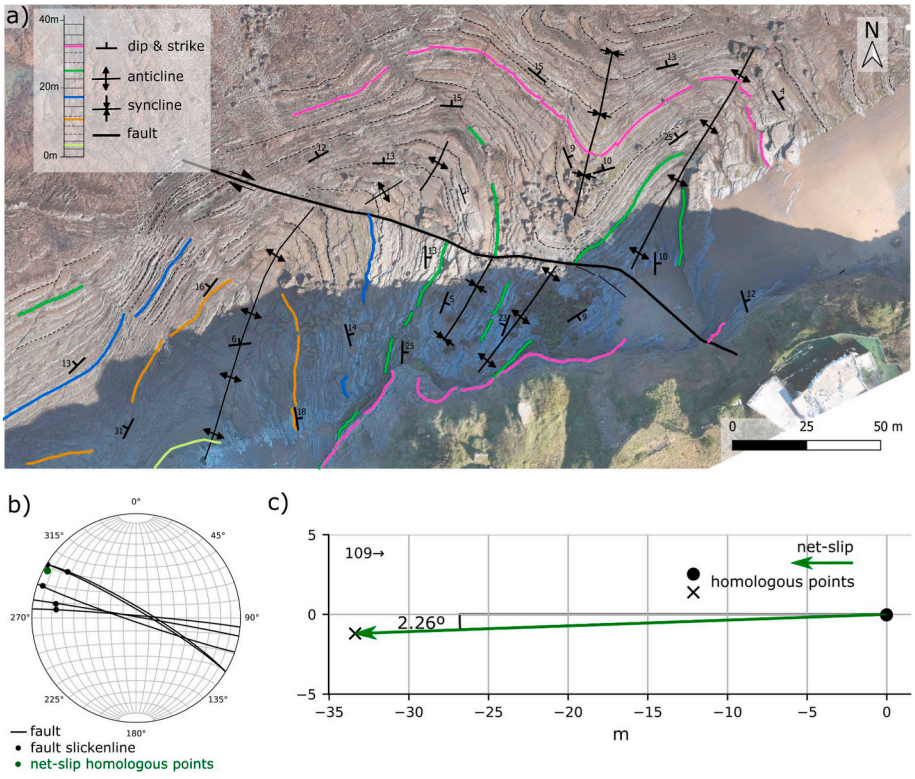

Fig. 10. a) Photogeological interpretation of an orthophotograph showing a WNW-ESE right-lateral strike-slip fault cutting and offsetting several NE-SW folds. b) Equal-area projection of measurements related to the fault shown in a), constructed with a Python script. c) Fault surface view showing the position of two homologous points in both fault blocks and the net-slip vector. The cross is located in the southern fault block, whereas the circle is located in the northern fault block. The homologous points have been obtained from the intersection of the fault surface with the axis of the same fold developed in the same layers. The fold used for the calculation is the easternmost anticline in figure a) and its axis has been calculated using the green horizon. (For interpretation of the references to colour in this figure legend, the reader is referred to the Web version of this article.)

motion pulses with not strictly parallel slickensides. The geological map shows that there are fault segments in which younger rocks are located in the northern block, i.e., the footwall, while older rocks are located in the southern block, i.e., the hanging wall, and therefore, the fault would behave as an apparent reverse fault (Fig. 11). However, there are segments where the opposite situation occurs, i.e., older rocks located in the northern fault block (footwall) are directly in contact with younger rocks located in the southern fault block (hanging wall), and thus the fault would behave apparently as a normal fault (Fig. 11). The segments where the fault acts as an apparent reverse fault and those where it acts as an apparent normal fault are separated by null points (term adapted from Williams et al., 1989, originally applied to inversion tectonics) in which the outcropping layers in the northern and southern fault blocks have the same age, and therefore, no strike separation occurs at these points. The calculated pitch of the net slip, pitch of the axial plane cut-off lines on the fault plane, the strike separation and the distance between fold hinges displaced by this fault have been plotted on the graphs in Figs. 8 and 9. On the one hand, the graph in Fig. 8 verifies that this fault shows apparently reverse and apparently normal segments along strike, as expected, since the slip vector and the axial plane cut-off lines are not parallel. On the other hand, the graph in Fig. 9 tells us that the width of the apparently reverse and apparently normal fault segments should be slightly greater than 30 m in the eastern portion of the fault and slightly greater than 10 m in the western part of the fault, as shown in the geological map (Fig. 10a).

4. Applications

From our point of view, the graphs presented here can be used in different ways.

1) As a tool to improve our structural interpretations in cases where observations are apparently contradictory. For example, if we see a reverse fault on a slope and a fault with strike-slip kinematic indicators on a flat region but the outcrops between the slope and the flat area are covered by vegetation, we may conclude that they are two different faults. Alternatively, if we see a strike-slip fault in a flat region and its continuation on the slope becomes a reverse fault, we may conclude that it is a reactivated fault. In these cases, the graphs presented can help us to determine whether they are indeed two different faults or they are the same fault in the first example, and whether it is a reactivated fault or it fits an interpretation based on a single movement in the second example.
2) From the predictive point of view in regions where we know that faults cut and offset previously tilted and/or folded layers. Thus, if we have information in geological map format as well as fault kinematic indicators, the graphs can help us to predict what type of fault dip separation will be expected in geological cross-sections. In the same way, if the information we have comes from sections across faults based on outcrops in road slopes, cliffs, mountain slopes, etc. the graphs can be useful to construct the geological map since they will allow us to infer what type of strike separation will be expected for the faults. If fault kinematic indicators are not available in the study area, the graphs could be used to constrain possible pitches of the net slip as long as the orientation of the fault plane and the layers, as well as geological cross-sections and map views of the faults, are available. This exercise could be also carried out using 3D seismic data. The procedure would consist of calculating the pitch of the bedding cut-off lines from the orientation of the layers and the fault. Next, determine the type of fault dip separation in cross section (normal, reverse or no separation) and the type of fault strike separation on the map (left, right or no separation). Next, a horizontal line corresponding to the pitch of the bedding cut-off lines should be drawn on the graphs of Fig. 2b and c only in the fields whose type of dip and strike separation coincides with the type of dip and strike separations determined. The horizontal line segments whose position is identical in both graphs will give us possible values of net-slip pitch and possible types of faults.
3) To check whether in a region the layers were tilted and/or folded before fault development. For instance, if the kinematic indicators tell us that a fault is a strike-slip fault, but the same fault appears as a reverse fault in cross section or it displays apparent reverse or normal segments along its map trace, the graphs might be used to check whether the type of fault determined based on the kinematic indicators is consistent with the type of dip and strike separation observed in the geological cross-sections and maps. If so, this confirms the presence of tilted and/or folded layers before fault development. If not, another hypothesis needs to be formulated.

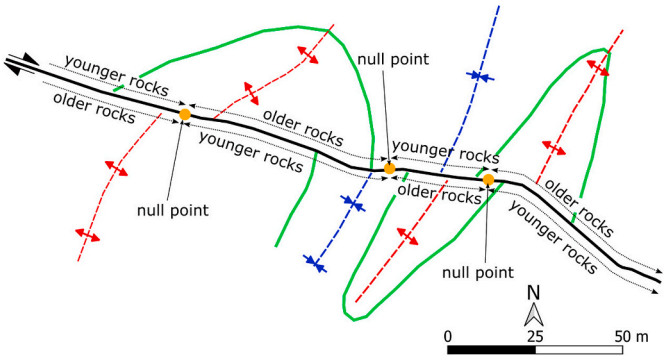

Fig. 11. Structural sketch of the fault illustrated in Fig. 10 showing the apparently reverse and apparently normal segments of the fault, as well as the null points. The fault trace exhibits a variable character as predicted by the graph in Fig. 8. The width of the apparently reverse and apparently normal fault segments is predicted approximately by the graph in Fig. 9a.

5. Conclusions

A correct classification of faults, based on their kinematics, requires a three-dimensional thinking. However, data are commonly obtained in two dimensions, and therefore, it is necessary to analyse geological maps and cross-sections when trying to unravel the structural history of a region. This type of exercise is usually carried out to decipher the fault type when no kinematic indicators are available. However, this analysis is not usually performed when kinematic elements are available, such as fault striations, homologous points on both fault blocks, etc., since they provide us incontestable information about the movement along faults, and therefore, we are generally satisfied with this information. What we want to emphasise here is that we recommend to carry out analyses of geological maps and sections across faults also in those cases where kinematic indicators associated with fault motion are available, as both are complementary techniques and may supply additional information.

Furthermore, although geological maps and sections are very old techniques, this work shows that they are still essential tools not only for the representation, visualization and understanding of the structure of a region, but also for deciphering the occurrence of deformational events prior to the development of faults.

This work is a first approach to the problem of apparently confusing situations in faults that cut and offset previously tilted and/or folded layers. However, to understand the full spectrum of possibilities there are still many parameters to be explored, such as the variation of fault slip along dip and/or strike, different geometries of folds or folds with inverted limbs amongst other parameters.

Credit author statement

Marta Magán: Methodology, Software, Validation, Investigation, Resources, Writing – review & editing, Visualization.

Josep Poblet: Conceptualization, Methodology, Validation,

Investigation, Resources, Writing - original draft, Writing – review & editing, Supervision, Project administration, Funding acquisition.

Mayte Bulnes: Methodology, Validation, Investigation, Resources, Writing – review & editing, Visualization, Supervision, Project administration, Funding acquisition.

Declaration of competing interest

The authors declare that they have no known competing financial interests or personal relationships that could have appeared to influence the work reported in this paper.

Acknowledgements

The authors would like to acknowledge financial support by research project CGL2015-66997-R, funded by the Spanish Ministry of Economy and Competitivity and the European Fund for Regional Development (FEDER), research project PID2021-126357NB-100, funded by the Spanish Ministry for Science and Innovation, research project FC-GRUPIN-IDI/2018/000216, funded by the Asturias Government, research contracts CN-16-014, CN-16-015 and CN-16-016, funded by Repsol Exploración S.A., and The Andrew Whitham CASP Fieldwork Award 2019. Marta Magán thanks the Severo Ochoa grant awarded by the Asturias Government. We acknowledge Petroleum Exploration Experts for the academic licenses to use the software Move. We thank the editor Ian Alsop and the reviewers Hodei Uzkeda and Massimiliano Masini for their useful comments and suggestions, Nilo Bobillo-Ares for helping us with mathematical issues, and José Carlos García-Ramos and Laura Piñuela for their help to identify the Jurassic stratigraphic sequences.

References

Allan, U.S., 1989. Model for hydrocarbon migration and entrapment within faulted structures. AAPG (Am. Assoc. Pet. Geol.) Bull. 73 (7), 803–811.

Beroiz, C., Ramírez del Pozo, J., Giannini, G., Barón, A., Julivert, M., Truyols, J., 1972. Mapa geológico de España, E. 1:50.000, Hoja 14 (13-3). Gijón. Instituto Geológico y Minero de España, Madrid.

Billings, M.P., 1972. Structural Geology. Prentice-Hall, Englewood Cliffs.

Crowell, J.C., 1959. Problems of fault nomenclature. AAPG (Am. Assoc. Pet. Geol.) Bull. 43 (11), 2653–2674.

Gutiérrez Claverol, M., Torres Alonso, M., Luque Cabal, C., 2002. El subsuelo de Gijón. Aspectos geológicos. CQ Licer S.L. Librería Cervantes, Oviedo.

Lepvrier, C., Martínez-García, E., 1990. Fault development and stress evolution of the post-Hercynian Asturian Basin (Asturias and Cantabria, northwestern Spain). Tectonophysics 184 (3–4), 345–356.

Martín, S., Uzkeda, H., Poblet, J., Bulnes, M., Rubio, R., 2013. Construction of accurate geological cross-sections along trenches, cliffs and mountain slopes using photogrammetry. Comput. Geosci. 51, 90–100.

Merino-Tomé, O., Suárez-Rodríguez, A., Alonso, J.L., 2014. Mapa geológico digital continuo a escala 1:50.000 de la Zona Cantábrica (Plan GEODE). http://info.igme.es/visor web.

Odriozola, M.J., 2016. Extensión y compresión en los materiales jurásicos de la playa de Peñarrubia. Gijón. MSc Thesis, Universidad de Oviedo.

Ragan, D.M., 2009. Structural Geology: an Introduction to Geometrical Techniques. Cambridge University Press, Cambridge.

Reid, H.F., Davis, W.M., Lawson, A.C., Ransome, F.L., 1913. Report of the committee on the nomenclature of faults. Bull. Geol. Soc. Am. 24 (1), 163–186.

Straley III, H.W., 1934. Some notes on the nomenclature of faults. J. Geol. 42 (7), 756–763.

Uzkeda, H., 2013. Reconstrucción 3D y análisis estructural de las rocas jurásicas de Colunga-Tazones (Cuenca Asturiana, NO de la Península Ibérica). PhD Thesis. Universidad de Oviedo.

Uzkeda, H., Bulnes, M., Poblet, J., García-Ramos, J.C., Piñuela, L., 2013. Buttressing and reverse reactivation of a normal fault in the Jurassic rocks of the Asturian Basin, NW Iberian Peninsula. Tectonophysics 599, 117–134.

Uzkeda, H., Bulnes, M., Poblet, J., García-Ramos, J.C., Piñuela, L., 2016. Jurassic extension and Cenozoic inversion tectonics in the Asturian Basin, NW Iberian Peninsula: 3D structural model and kinematic evolution. J. Struct. Geol. 90, 157–176.

Uzkeda, H., Poblet, J., Bulnes, M., Martín, S., 2018. Effects of inherited structures on inversion tectonics: examples from the Asturian basin (NW Iberian Peninsula) interpreted in a Computer assisted virtual environment (CAVE). Geosphere 14 (4), 1635–1656.

Uzkeda, H., Poblet, J., Magán, M., Bulnes, M., Martín, S., Fernández-Martínez, D., 2022. Virtual outcrop models: digital techniques and an inventory of structural models from north-northwest Iberia (Cantabrian zone and Asturian basin). J. Struct. Geol. 157, 104568.

Williams, G.D., Powell, C.M., Cooper, M.A., 1989. Geometry and kinematics of inversion tectonics. In: Cooper, M.A., Williams, G.D. (Eds.), Inversion Tectonics, vol. 44. Geological Society, London, Special Publications, pp. 3–15.

Xu, X., Aiken, C.L., Bhattacharya, J.P., Corbeanu, R.M., Nielsen, K.C., McMechan, G.A., Abdelsalam, M.G., 2000. Creating virtual 3-D outcrop. Lead. Edge 19 (2), 197–202.